

# Recent Charm Hadroproduction Results from Fixed Target Experiments

---

**J. S. Russ**

*Carnegie Mellon University*

*Pittsburgh, PA 15213 USA*

*Email: russ@cmphys.phys.cmu.edu*

ABSTRACT: A number of new experimental results on charm hadroproduction from pion beams and, recently, proton and  $\Sigma^-$  beams have been presented. This review compares recent results, including new photoproduction results, and comments on some questions they raise.

## 1. Introduction

The study of charm hadroproduction processes has been carried out for the past 2 decades, with the goal of testing ideas of perturbative QCD at the charm quark mass scale. The issues involved in these studies, as outlined in Nason's paper in these proceedings [1], are rather complicated for charm. At the quark level they involve choices of:

- renormalization scale for the quark-level process
- factorization scale for the parton distributions
- quark constituent mass, to sum over gluon effects implicit in the factorized form
- intrinsic charm quark constituents in the beam or target wave function
- intrinsic transverse momentum  $k_T$  in the scattering due to confinement effects

Since the actual observables are the color-singlet final state hadrons, one must add non-perturbative estimates of hadronization effects:

- color-drag effects between either the  $c$  or  $\bar{c}$  quark and the outgoing colored fragment from the beam or target hadron.

- other hadronization effects, including rescattering of the separating charmed and anti-charmed hadrons.

The goal of the latest round of charm hadroproduction experiments is to compare production of several charm species at different energies by several different beam hadrons. One can test:

- hadronization effects in the  $p_T$  spectrum
- hadronization and  $k_T$  effects in charm pair production
- color-drag effects and  $x_F$  dependence versus charm type
- $c\bar{c}$  asymmetries for various beam hadrons

For this review the new data to be considered comes from the following experiments:

- WA92 [2] (340 GeV/c  $\pi^-$ )
- E791 [3] (500 GeV/c  $\pi^-$ )
- WA89 [4] (340 GeV/c  $\Sigma^-$ )
- SELEX [5] (600 GeV/c  $\pi^-, \Sigma^-, p$ )
- FOCUS [6] (220 GeV/c  $\gamma$ )

## 2. General Theoretical Features of Charm Hadroproduction

Within the framework of leading order (LO) QCD calculations the general features of hadroproduction can be represented schematically as shown in figure 1. This simplified picture uses factor-

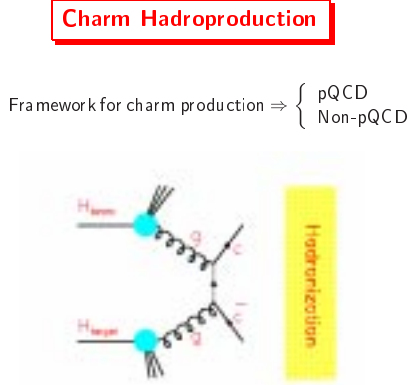


**Figure 1:** Schematic of charm hadroproduction process

ization to separate the hard scattering process of charm production from the parton production characteristics that may vary from hadron to hadron. The charm quark constituent mass is a parameter of the theory. One might ask whether it is the same for all charmed hadrons, since the constituent mass includes effects from the local gluon fields. Heavy Quark Effective Theory arguments favor a single constituent mass, since the heavy quark fields are decoupled from the light quark degrees of freedom. Testing any such variation in the data is not simple. A variation in the constituent mass between mesons and baryons, for example, would change the meson/baryon production ratio. However, this ratio is sensitive to other hadronization effects that surely will mask those due to a variation in the constituent mass. We will not consider this question further.

NOT shown in this simple diagram are extra complications as discussed in more detail by Nason, using the general procedure of [7]:

- NLO gluon radiation
- initial-state  $\overline{k_T}$  effects

It is a striking feature of these NLO calculations that the single charm differential distributions

are not changed in shape but only in normalization. Only in the azimuthal angle distribution  $\mathbf{p_{T1}} \cdot \mathbf{p_{T2}}$  for charm pairs is there an obvious effect of the extra gluon kinematics, as will be discussed later.

NLO effects are also built into the simulation code PYTHIA [8] within the framework of a color string model. As we shall see, the MNR (Mangano, Nason, and Ridolfi) code tends to represent the data better in general than the Pythia code with default parameters.

## 3. $p_T^2$ Distributions and Hadronization Effects

Theoretically, it is clear that the distributions in  $x_F$  and  $p_T$  for charm hadrons should be softer than the  $c\bar{c}$  distributions due to fragmentation effects ... unless they are harder because of color-drag or intrinsic charm effects. Typically fragmentation is treated using the empirical Peterson function. [9] Most charm hadroproduction data match better to bare quark distributions than to a typical hadronized form. Consequently, in the analyses to be discussed below, the Peterson parameter  $\epsilon$  is varied in the range 0.01-0.06, the hard fragmentation limit. Questions about the hadronization process to be considered from the experimental side include:

- Can the effects be calculated?
- Are they universal for all charm or species-dependent?
- In which parameters are the effects most clearly measureable?

### 3.1 Charm Meson Production in $\pi^-$ Beams

Two recent pion experiments have reported measurements of the  $p_T$  distributions for D meson production. WA92 presented the combined spectrum for both neutral and charged states, combining particle and antiparticle. The range of  $p_T^2$  is large, extending to about 20 (GeV/c)<sup>2</sup>. They compare to a calculation using the MNR code without hadronization and report a good match, as seen in figure 2.

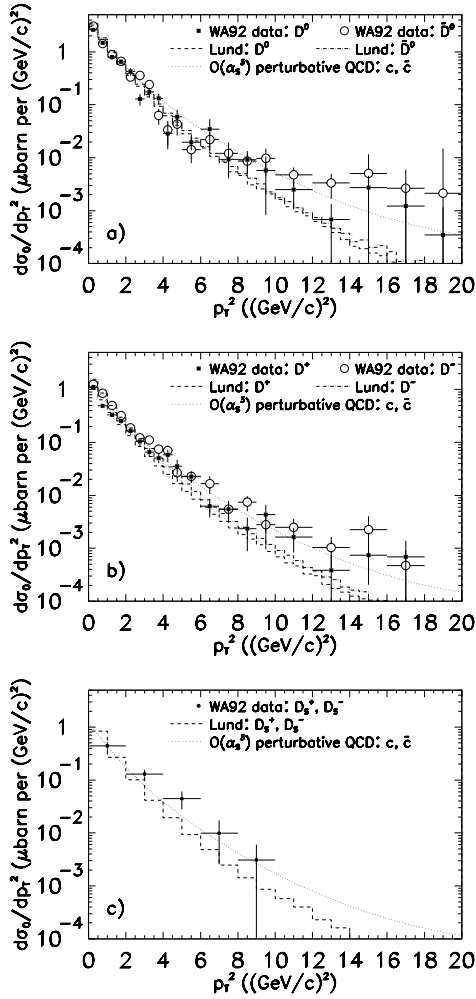


Figure 2: WA92  $D^{0,+}$  + c.c.  $p_T^2$  distribution (350 GeV/c  $\pi^-$ )

E791 has much higher statistics (20x more data than WA92) in their 500 GeV/c experiment. They present a study of the  $p_T^2$  distribution for  $D^0$  mesons [ + c.c.] covering approximately the same range in  $p_T^2$  as WA92. They see clearly the change in slope at higher  $p_T$  that is expected in the parton picture. figure 3 shows the MNR  $O(\alpha_s^3)$  calculation with and without hadronization, as well as to two PYTHIA models. It is very exciting to see that hadronization effects may for the first time be detectable in the data. E791 shows that the MNR computation with hadronization gives a better match to the behaviour at small  $p_T$  than the bare-quark calculation. There is little difference between the two in the large- $p_T$  tail. The exact details of

the shift from bare quark to hadronized single-particle distributions are not simple to extract from the MNR code. It's an interesting question to ask where the corresponding hadronization effects will show up in the b-quark sector. Are the collider experiments, with a relatively large  $(p_T)_{\min}$  cutoff, sensitive to the difference between bare-quark and hadronized shapes?

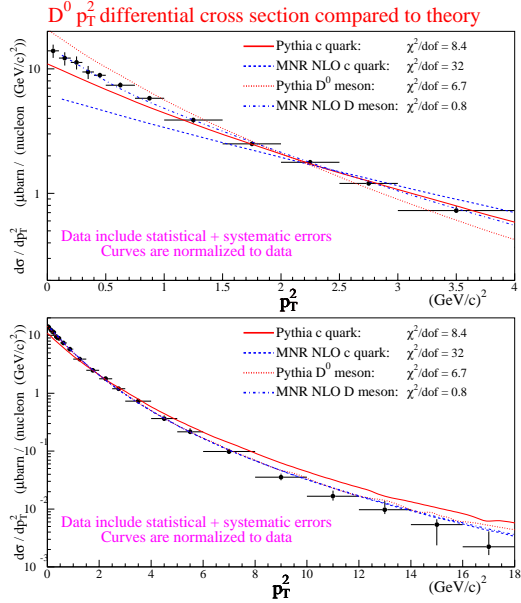


Figure 3: E791  $D^0$  + c.c.  $p_T^2$  distribution (500 GeV/c  $\pi^-$ )

For pion production the  $p_T^2$  spectra from both E791 exclusive  $D^0$  and WA92 combined  $D^0$  and  $D^+$  studies show a clear break in slope for  $p_T^2 \sim 6$  (GeV/c) $^2$ . The large  $p_T^2$  behaviour agrees with  $O(\alpha_s^3)$  calculation.

### 3.2 Charm Baryon Production

The SELEX experiment has data in the same spectrometer for incident  $\pi^-$ ,  $\Sigma^-$ , and proton beams. Figure 4 shows the  $p_T^2$  distributions for  $\Lambda_c^+$  production by each of the 3 beam particles. These comparisons can be sensitive, for example, to hadron size effects as reflected in the  $k_T$  parameters needed to fit the different spectra.

The mean  $p_T^2$  values for  $\Lambda_c^+$  production by all 3 beam hadrons in SELEX at 600 GeV/c are similar to those for  $D^0$  production reported by E791 for a 500 GeV/c  $\pi^-$  beam. The SELEX  $\Sigma^-$  data show a slope change near  $p_T^2 \sim 4$  (GeV/c) $^2$ , also

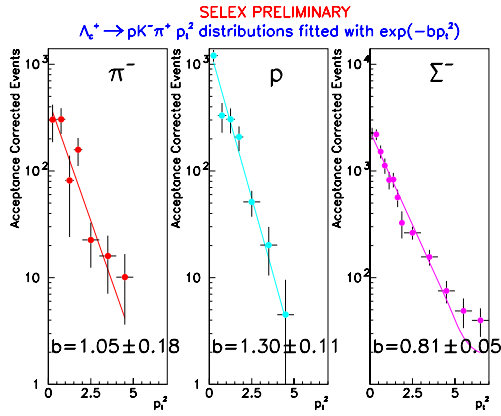


**Figure 4:** SELEX  $\Lambda_c^+$  (no c.c.)  $p_T^2$  distributions (600 GeV/c)

similar to D meson data with a  $\pi^-$  beam. [2, 3] The SELEX experimenters have not yet made model fits to their data, in part because of the problem of describing the s-quark structure function in the  $\Sigma^-$  beam.

#### 4. Charm Pair Analyses

Additional information about the smearing effects of the intrinsic  $k_T$  distributions of the partons and NLO gluon radiation comes from charm pair distributions. Until recently, there were few fully-reconstructed charm pairs in hadroproduction data. There are now new results from E791 (hadroproduction) and FOCUS (photoproduction) on pairs of D mesons. The E791 analysis has made an extensive study of the pair correlations in  $x_F$ ,  $p_T$ ,  $\Delta y$ , and mass. Correlations in almost all variables are rather weak, dominated by kinematics, *except* for the  $\Delta\phi$  distributions of the transverse momentum vectors of the pair. In LO QCD, this should be a  $\delta$  function at  $180^\circ$ . The  $\Delta\phi$  distribution in figure 5 is very flat, flatter than calculated from NLO QCD. This may be due to other non-perturbative effects (intrinsic  $k_T$ ) or it may arise via final state interactions after hadronization.

Let me reach slightly outside the strict definition of hadroproduction to include in this review some beautiful new photoproduction data on D meson pairs from FOCUS. In this preliminary sample, they demonstrate their overwhelm-

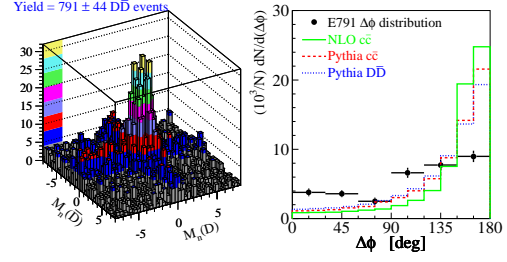


**Figure 5:** D Pair Characteristics from E791 (500 GeV/c  $\pi^-$ )

ing statistics, showing 7000 reconstructed pairs in the preliminary analysis. They have not had time to make a complete study of the correlations. Figure 6 shows that for photoproduction, in striking contrast to the E791 hadroproduction data, the pair  $\Delta\phi$  distribution is mostly back-to-back, with a modest tail from smearing processes. In photoproduction, the NLO gluon emission is reduced and there is lower  $k_T$ . Any final state interaction effects after hadronization would be essentially the same here as in hadroproduction. The FOCUS data tend to argue against final state interactions as the source of the broadened pair  $\Delta\phi$  distribution.

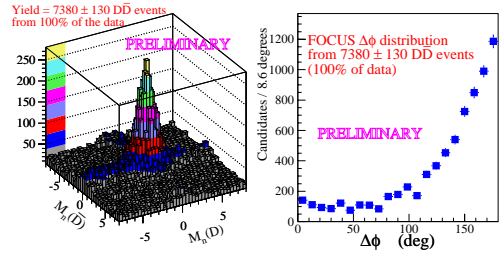


**Figure 6:** D Pair Characteristics from FOCUS (Photoproduction)

#### 4.1 $p_T^2$ Summary for D Mesons, $\Lambda_c^+$

The  $p_T^2$  distribution for both D mesons and  $\Lambda_c^+$  baryons shows a transition from the usual forward exponential behavior to a slower decrease near  $p_T^2 \sim 4-6$  (GeV/c) $^2$ . The meson data are pion produced, while the baryons are principally hyperon-produced. Are the slight differences in exponential slope and break point important or

not? If one takes them seriously, they may suggest either different geometric size for charm baryons or mesons or different  $k_T$  effects for pions and hyperons due to the different hadron radii. The D-pair  $\Delta\phi$  distributions for pion-production and photoproduction are strikingly different, raising again the question of whether the idea of intrinsic  $k_T$  is necessary for photoproduction. For pion-production, can a single value of intrinsic  $k_T$  explain both the single-charm  $p_T^2$  distribution and the D-pair  $\Delta\phi$  results?

## 5. New $x_F$ Analyses

The description of the longitudinal momentum distribution for charm production is traditionally given in terms of the Feynman  $x_F$  variable, the fraction of the total available center-of-mass (CM) momentum carried off by the outgoing parton, or in these cases, the outgoing charm hadron. The choice of functional form is somewhat arbitrary. The distribution usually is parametrized as  $(1 - x_F)^n$ , where  $x_F$  is calculated in terms of the the outgoing longitudinal CM momentum of the charm state and the invariant CM energy  $\sqrt{s}$ :

$$x_F = 2p_{\parallel}^*/\sqrt{s}$$

We note that this definition of  $x_F$  is useful for most of the observable  $x_F$  regime, but it may not be appropriate when  $x_F \rightarrow 1$ . In that case, the maximum CM momentum may depend in an important way on the effective mass of the charmed pair, since the charm system will carry off most of the available CM energy. This issue has not been discussed heretofore in the literature, but some of the new data from SELEX begins to raise the question.

$x_F$  distributions for charm hadrons are often analyzed for **leading particle** effects. The customary definition of a leading hadron is one which shares at least one valence quark with the beam hadron. In color-drag analyses leading behaviour shows up primarily at large  $x_F$  and leads to enhanced production of the leading species compared to the non-leading species, i.e., to an asymmetry. The leading charm hadron is also expected to show a harder  $x_F$  distribution than

its non-leading partner. The new SELEX data challenge these expectations.

### 5.1 $D^0$ Mesons

SELEX and E791 both have new analyses of combined  $D^0 + c.c.$   $x_F$  distribution from pions. Figure 7 shows the SELEX data and a scaled subset of the E791 results. The two experiments generally agree well. The E791 point at largest  $x_F$  lies above the trend of the data. SELEX data tend to lie closer to a simple  $(1 - x_F)^n$  curve, with no rise at the largest values. The E791 point has quite an asymmetric error; the scaled value in the  $x_F$  bin 0.6-0.8 is  $102^{+23}_{-50}$  units. The SELEX data, if combined, gives  $32 \pm 10$  units in the same bin. These are statistically consistent, of course. One may combine them to suggest there is little, if any, rise at large  $x_F$  for  $D^0$  production.

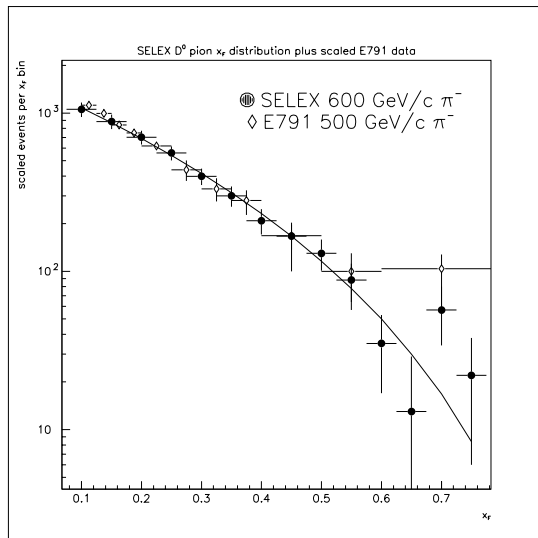


**Figure 7:**  $x_F$  distribution for  $D^0 + c.c.$  from SELEX and E791

The E791 measurement was designed to explore the systematics of hadroproduction near  $x_F = 0$ . They succeeded admirably in this goal. Their full data set, shown in figure 8, show a shift of the  $x_F$  distribution's peak toward positive  $x_F$  for the  $\pi^-$  beam. This is consistent with a larger momentum fraction for partons in the  $q\bar{q}$  hadron than in the  $qqq$  hadron, resulting in movement of the production CM system in the direction of the beam particle in the laboratory.

The E791 analysis has compared the experimental  $x_F$  distributions to those expected from

the MNR model and PYTHIA calculations. Again, the calculated distributions are sensitive to the inclusion of hadronization effects. Unlike the E791  $p_T^2$  data, their  $x_F$  data show better agreement with the MNR  $c\bar{c}$  calculation than with the hadronized version. The good news is that these distributions are sensitive to hadronization effects. The bad news is that current model calculations cannot describe both  $x_F$  and  $p_T$  distributions simultaneously.

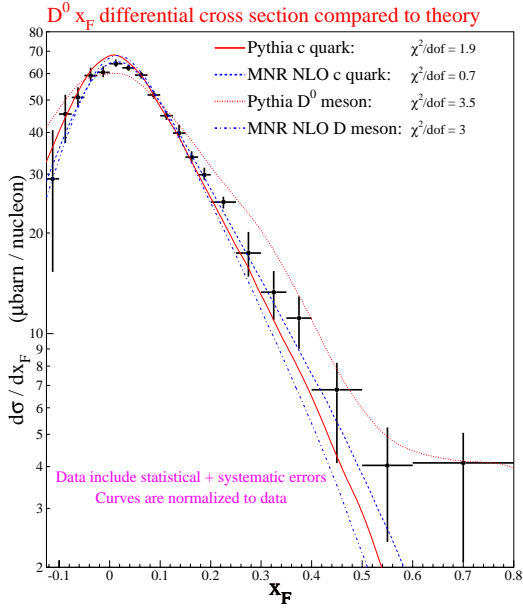


Figure 8:  $x_F$  distribution for  $D^0 + c.c.$  E791

SELEX looks at the  $x_F$  dependence for  $D^0$  and  $\bar{D}^0$  separately. There is a complication in these distributions from feed-down from  $D^{*+}$ . No  $D^*$  removal is made in the SELEX data, summarized in figure 9.

The various  $x_F$  distributions all fit to the standard form  $(1 - x_F)^n$  with reasonable  $\chi^2$  values. Table 1 summarizes the results. One sees from table 1 that the  $n$ -dependence is very different for the baryon beams (no valence antiquarks) compared to the  $\pi^-$  beam, for which the  $D^0$  is leading. In the SELEX pion data there is a significantly harder  $x_F$  distribution for the leading particle compared to the non-leading. However, the yields of both particles for  $x_F \geq 0.3$  are quite comparable. The SELEX apparatus acceptances are the same for  $c$  and  $\bar{c}$  states. The difference in the power-law behavior arises from increased

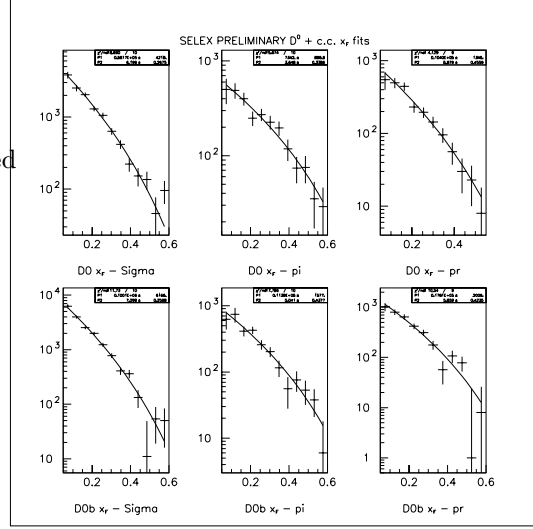


Figure 9: SELEX  $x_F$  distribution for  $D^0$  and  $\bar{D}^0$

$\bar{D}^0$  production at small  $x_F$  compared to  $D^0$  production. I conclude that the differences in the pion  $x_F$  distributions are unlikely to be related to color-drag.

Meson	Beam	expt	$n$	$x_F$ range
$D^0 + \bar{D}^0$	$\pi^-$	E791	$4.61 \pm .19$	.05-.50
all D and $\bar{D}$	$\pi^-$	WA92	$4.27 \pm .11$	0-.08
$D^0$	$\pi^-$	SELEX	$3.65 \pm .35$	0.1-0.65
$\bar{D}^0$	$\pi^-$	SELEX	$5.04 \pm .44$	0.1-0.65
$D^0$	p	SELEX	$5.88 \pm .46$	0.1-0.65
$\bar{D}^0$	p	SELEX	$5.86 \pm .43$	0.1-0.65
$D^0$	$\Sigma^-$	SELEX	$6.20 \pm .27$	0.1-0.65
$\bar{D}^0$	$\Sigma^-$	SELEX	$7.30 \pm .26$	0.1-0.65

Table 1: SELEX  $D^0$  and  $\bar{D}^0$   $x_F$  distributions fit to  $(1 - x_F)^n$

For protons, the  $\bar{D}^0$  meson shares a u quark in common with the beam. The  $x_F$  distributions for the particle and antiparticle are very similar for the proton beam. The power law fits give the same  $n$  values, and all parts of the  $x_F$  distribution favor  $\bar{D}^0$  production by about the same ratio. This is not how color-drag is supposed to work. SELEX concludes that neither pion nor proton production of  $D^0$  mesons shows a leading effect.

## 5.2 $D^\pm$ Mesons

SELEX has new data on the hadroproduction of charged D mesons by  $\pi^-$ ,  $\Sigma^-$  and proton beams. Figure 10 shows results that are quite comparable to those for the neutral D mesons, namely, very similar distributions with the same n value for the two baryon beams, and a somewhat harder spectrum for the pion beam. The  $D^-$  shares a valence quark with all 3 beam hadrons, but there is little evidence of color-drag effects in the distributions. The overall yield for  $D^-$  is higher at all  $x_F$  in all cases. For the  $\pi^-$  beam, the  $D^+$  distribution is actually harder than the  $D^-$  distribution. The n values are summarized in table 2.

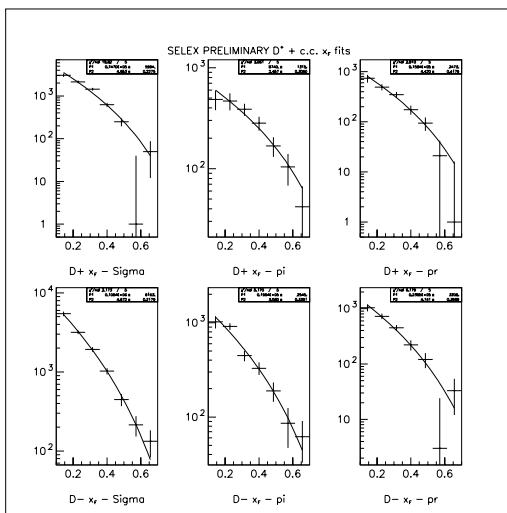


Figure 10: SELEX  $D^\pm \rightarrow K\pi\pi$   $x_F$  distribution

Meson	Beam	$n$	$x_F$ range
$D^+$	$\pi^-$	$2.46 \pm .31$	0.1-0.7
$D^-$	$\pi^-$	$3.58 \pm .34$	0.1-0.7
$D^+$	p	$4.42 \pm .42$	0.1-0.7
$D^-$	p	$4.74 \pm .40$	0.1-0.7
$D^+$	$\Sigma^-$	$4.95 \pm .23$	0.1-0.7
$D^-$	$\Sigma^-$	$4.67 \pm .22$	0.1-0.7

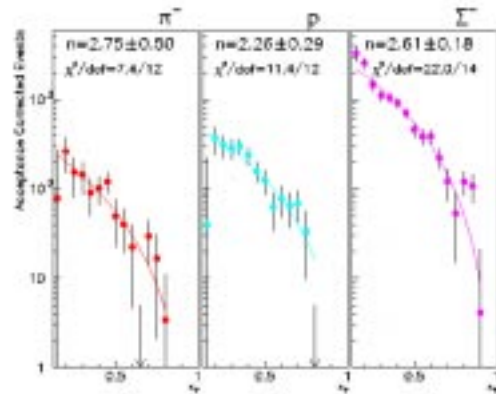
Table 2: SELEX  $D^+$  and  $D^-$   $x_F$  distributions fit to  $(1 - x_F)^n$

## 5.3 $\Lambda_c^+$ Baryons

SELEX also has new data on  $\Lambda_c^+$  and  $\Lambda_c^-$  production by  $\pi^-$ ,  $\Sigma^-$  and p beams. For  $\Lambda_c^+$  production,

all 3 beam hadrons share a valence quark in common with the final state. The n-values for all 3 fits to the  $x_F$  distributions are comparable within errors and indicate that  $\Lambda_c^+$  production is quite hard. The data are shown in figure 11

### $x_F$ Distributions $\Lambda_c^+ \rightarrow pK^- \pi^+$



- $x_F$  Distributions for  $\pi^-$ , p, and  $\Sigma^-$  beams
- $\Lambda_c^+$  is a leading particle for all the 3 beam types

Figure 11:  $\Lambda_c^+$   $x_F$  dependence SELEX (600 GeV/c)

The high statistics  $\Sigma^-$  data do not fit well to the empirical function. There are apparent structures at both low and high  $x_F$ , as are emphasized in figure 12. The high  $x_F$  structure illustrates the need to understand how to compute  $x_F$  for hadronic states near the kinematic limit. The distribution may be distorted by having used the standard definition of  $x_F$ .

The  $\Lambda_c^-$  distributions are dramatically different from those of the  $\Lambda_c^+$  for baryon beams. In contrast, they are quite comparable for the pion beam. The baryon beams, with no valence anti-quarks in the fragmentation jet, have appreciable  $\Lambda_c^-$  production only at small  $x_F$ . The pion beam, conversely, makes copious  $\Lambda_c^-$  even at  $x_F \geq 0.4$ , comparable to the yield for  $\Lambda_c^+$ . This seems to be clearly related to a color-drag effect, since the spectator valence parton in the pion is equally-likely to be a q or a  $\bar{q}$ . Note that in these pion data the  $\Lambda_c^-$  finds a third  $\bar{q}$  at large  $x_F$  to form the antibaryon with about the same likelihood as

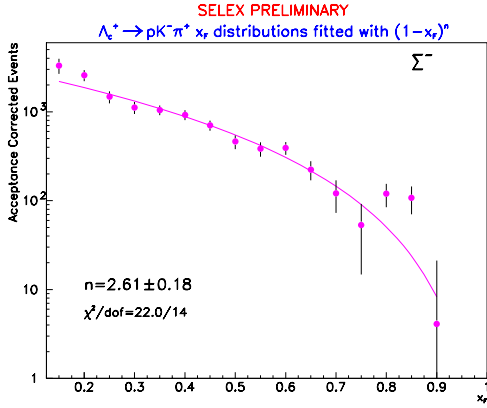


**Figure 12:** SELEX  $\Lambda_c^+$   $x_F$  dependence for 600 GeV/c  $\Sigma^-$

the  $\Lambda_c^+$  finds a third q at large  $x_F$ .

The  $x_F$  distributions for  $\Lambda_c^-$  are fitted to  $(1-x_F)^n$  forms and the results are shown in figure 13. Fits are summarized in table 3.

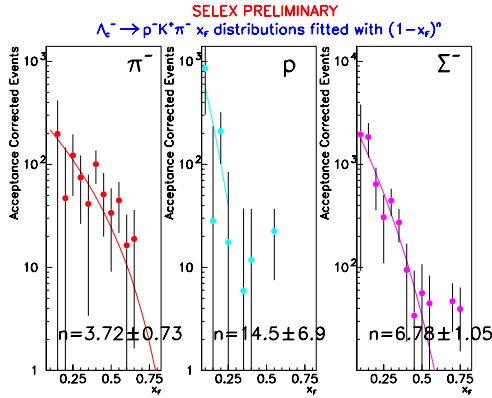


**Figure 13:**  $\Lambda_c^-$   $x_F$  dependence SELEX (600 GeV/c)

Baryon	Beam	$n$	$x_F$ range
$\Lambda_c^+$	$\pi^-$	$2.75 \pm .50$	0.15-0.8
$\Lambda_c^-$	$\pi^-$	$3.72 \pm .73$	0.15-0.65
$\Lambda_c^+$	p	$2.26 \pm .29$	0.15-0.8
$\Lambda_c^-$	p	$14.5 \pm 7$	0.15-0.65
$\Lambda_c^+$	$\Sigma^-$	$2.61 \pm .18$	0.15-0.9
$\Lambda_c^-$	$\Sigma^-$	$6.8 \pm 1.0$	0.1-0.65

**Table 3:** SELEX  $\Lambda_c^+$  and  $\Lambda_c^-$   $x_F$  distributions fit to  $(1-x_F)^n$

## 6. Recent Hadroproduction Asymmetry Studies

Recently attention has focussed on the issue of production asymmetry between charm and anti-charm states as part of the study of leading effects. To treat all charm on comparable footing, let us define the asymmetry A as:

$$A = \frac{N(\text{charm}) - N(\text{anticharm})}{N(\text{charm}) + N(\text{anticharm})}$$

The LO or even NLO charm production diagrams 1 show no particle/antiparticle asymmetry. The color-drag effects mentioned above are one mechanism for introducing an asymmetry. [10] The intrinsic-charm model [11] has a different asymmetry prediction. How do the new data compare to either of these ideas?

### 6.1 $\Lambda_c^+$ Asymmetry

WA89 ( $\Sigma^-$  beam) first showed an  $x_F$  distribution for  $\Lambda_c^+$  with a strong asymmetry (figure 14). The new SELEX data affirm that for the  $\Sigma^-$  beam and show that it's also true for a proton beam (figure 15).

The SELEX analysis makes a maximum likelihood fit to the asymmetry with no limit at  $A = \pm 1$ . This approach gives symmetric errors on points near the physical limit. The baryon-beam asymmetries are large at all  $x_F$ . The protons, especially, show significant  $\Lambda_c^-$  only in the small  $x_F$  region. The  $\Sigma^-$  data have a smoother approach of the asymmetry to the limit at +1.

In contrast to the baryon results, for  $\pi^-$  production the  $\Lambda_c^+$  asymmetry from SELEX is small and generally constant with  $x_F$ . This agrees well with new data from E791 (figure 16). In the central region E791 reports a small, positive  $\Lambda_c^+$  asymmetry that matches onto the SELEX data.

There is also new data from FOCUS on the first statistically-significant  $\Lambda_c^+$  asymmetry in photoproduction. The effect is small and independent of  $x_F$  (figure 17). The question is why is there an asymmetry at all in photoproduction. The photon-gluon fusion picture gives a production environment that is completely symmetric

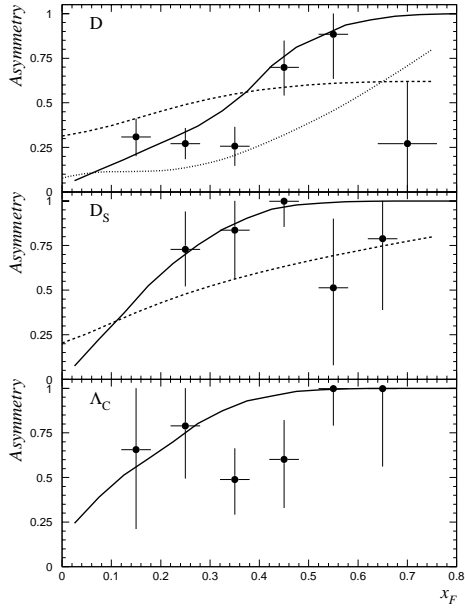


Figure 14: Charged Charm Asymmetries from WA89(340 GeV/c  $\Sigma^-$ )

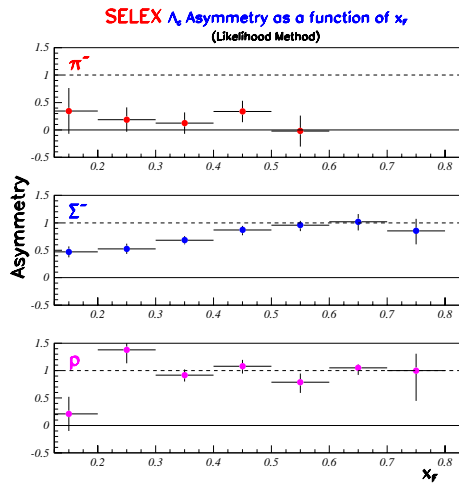


Figure 15:  $\Lambda_c^+$  Asymmetry from SELEX (600 GeV/c)

in  $q$  and  $\bar{q}$  distributions. Why should they be unbalanced? Whatever the cause, it does not depend on  $x_F$ .

### 6.2 Charged D Meson Asymmetry

The initial interest in charm asymmetry was stimulated by data from E791 and WA82, who reported a large  $x_F$ -dependent asymmetry for  $D^+$

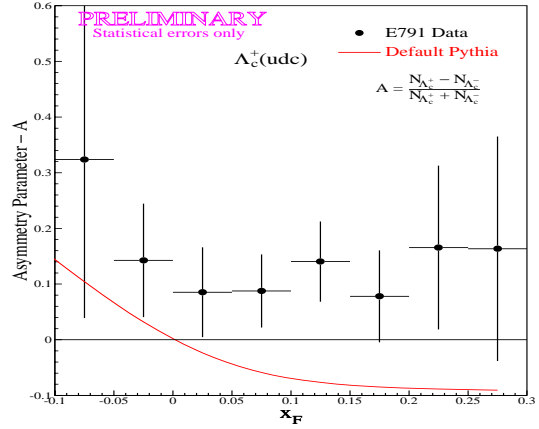


Figure 16:  $\Lambda_c^+$  Asymmetry from E791 (500 GeV/c  $\pi^-$ )

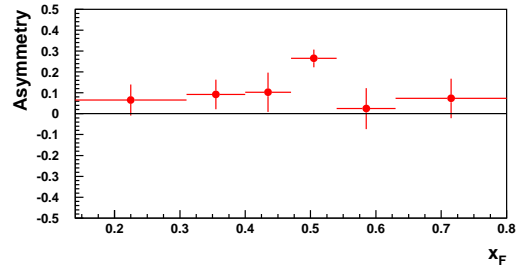


Figure 17: PRELIMINARY  $\Lambda_c^+$  Asymmetry from FOCUS (Photoproduction)

production by  $\pi^-$  at  $x_F \geq 0.4$ , as shown in figure 18.

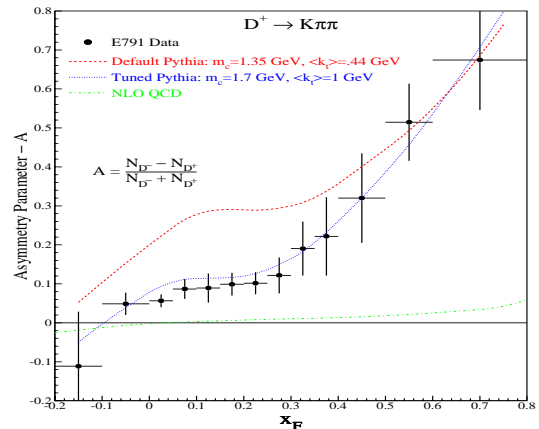
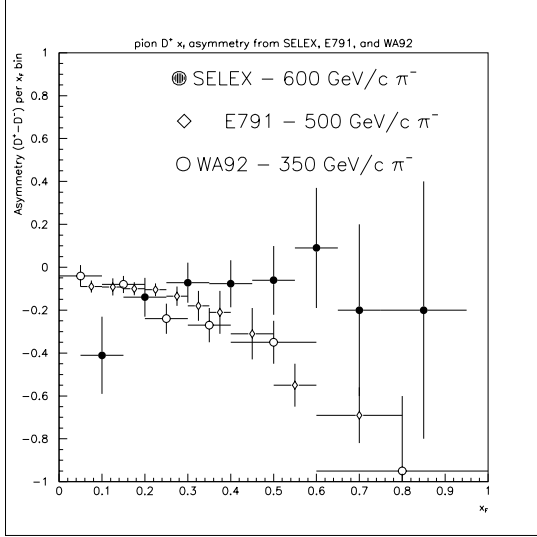


Figure 18:  $D^+$  Asymmetry from E791 (500 GeV/c  $\pi^-$ )

There are new data from WA92 and *prelim-*

inary SELEX results. We summarize the old E791 data and newer results in figure 19. The new SELEX data seems to disagree with the other results. Should they be believed?



**Figure 19:**  $D^+$  Asymmetry from E791, WA92, and SELEX

The disagreement affects the points at large  $x_F$ . The SELEX apparatus was optimized for this region, as one can see in figure 20, which shows that the mass resolution is independent of  $x_F$ . The SELEX acceptance is high out to  $x_F=1$  and charge-symmetric. For the other experiments the acceptance falls rapidly at large  $x_F$ , and the corrections are somewhat different for  $D^+$  and  $D^-$ . The SELEX pion data sample is statistically weaker than that of E791, but the trend of the distribution is clearly different and does not show a large asymmetry at high  $x_F$ . The SELEX analysis is continuing.

What about  $D^\pm$  meson production characteristics from beams besides  $\pi^-$ ? SELEX has new data comparing meson- and baryon-produced asymmetries. As can be seen in figure 21, all beams give similar, small asymmetries favoring  $\bar{c}$  states. There is little or no  $x_F$  dependence.

### 6.3 $D^0$ Asymmetries

The  $D^0$  distributions may be distorted by  $D^0$  states produced by the decay of  $D^*$  mesons. There is a recent report from WA92 about  $D^*$  production by  $350 \text{ GeV}/c \pi^-$ . [12] They report an asymmetry for the  $D^*$  consistent with 0 over the  $x_F$

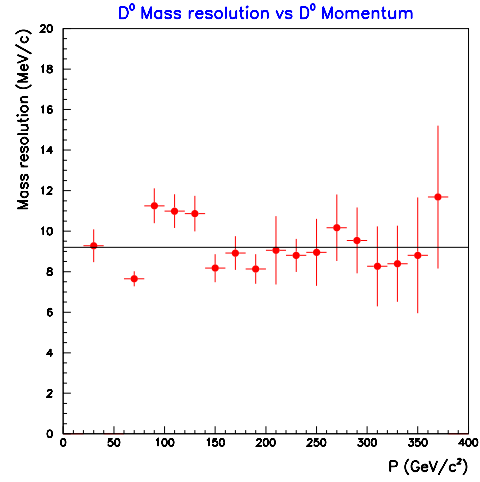


**Figure 20:** SELEX  $D^0 \rightarrow K\pi$  Gaussian mass width vs  $D^0$  momentum

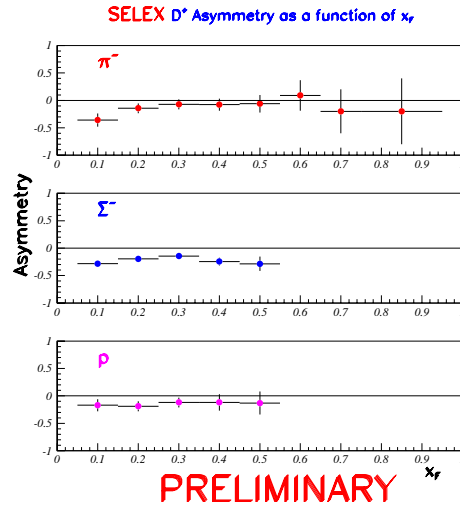


**Figure 21:** SELEX  $D^\pm \rightarrow K\pi\pi$  asymmetry

range 0.1-0.7. This is consistent with an earlier measurement at  $250 \text{ GeV}/c$  by E769. [13] Any intrinsic  $D^0$  asymmetry will therefore be reduced by  $D^0$  produced from  $D^*$  decays. From reference [12] the ratio of the inclusive  $D^0$  cross section to the inclusive  $D^{*+}$  cross section is  $2.42 \pm 0.13$  for  $x_F \geq 0$ , consistent with other results at lower energy. This says that the dilution of the  $D^0$  asymmetry by  $D^*$  effects is small.

The SELEX preliminary results for the  $D^0$  asymmetry from the 3 beam hadrons is shown in figure 22. The asymmetries in all cases are small

and relatively independent of  $x_F$ .

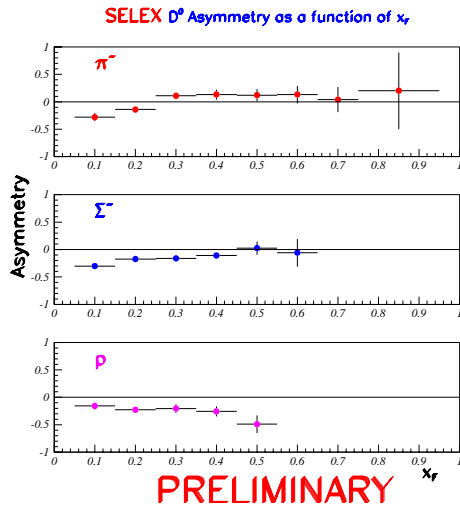


Figure 22: SELEX  $D^0$  asymmetry

If the  $D^0$  production spectrum is not distorted by feeddown from  $D^*$  decays, then in a  $\pi^-$  beam, which produces leading  $D^0$  and  $D^-$ , the  $D^0$  and  $D^+$  asymmetries should be equal and opposite. For SELEX figure 23 shows good agreement, supporting the picture of small asymmetry at large  $x_F$  for pion production of D mesons.

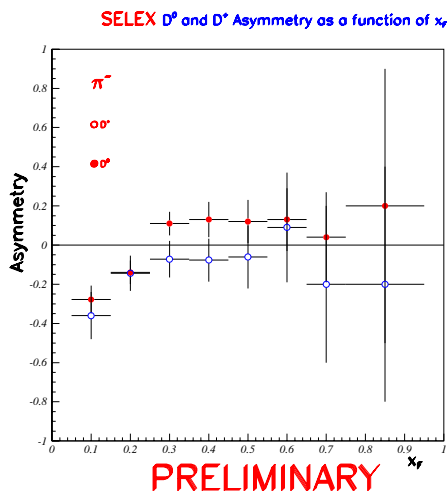


Figure 23: SELEX  $D^0$  and  $D^+$  asymmetry for  $\pi^-$  beam

## 7. Summary and Conclusions

In this last decade of fixed target charm experiments, we have seen new advances in comparisons of experiment and theory. E791 has shown that careful comparison of  $p_T^2$  and  $x_F$  distributions with model calculations may illuminate the hadronization puzzle for charm. In the current situation there are still inconsistencies to be resolved, but the work does illustrate potential sensitivity to the processes.

Lovely new charm pair data from E791 and FOCUS indicate significant differences between hadroproduction and photoproduction over the role of  $k_T$  and/or higher-order diagrams in determining the  $\Delta\phi$  distribution of the pairs. Recall that for single-charm  $p_T$  distributions, photoproduction analyses historically have preferred  $k_T$  to be small or 0, while hadroproduction has required  $k_T \sim 1-2$  GeV/c.

New  $\pi^-$  beam data from SELEX show a small  $D^+$  asymmetry at large  $x_F$ . SELEX asymmetries for D mesons are generally small and show little  $x_F$  dependence with any type of beam hadron. The SELEX data are self-consistent and raise questions about previous reports of a rising asymmetry at large  $x_F$  for the  $D^+$ . More work is required to understand the data.

The total  $x_F$  data with both pion and baryon beams do not yield a consistent picture of leading effects. Leading behavior is seen clearly in  $D_s^+$  and  $\Lambda_c^+$  production by baryon beams, for which  $x_F$  distributions are strongly asymmetric, favoring the leading species. However, for pion beams these same states show only weak leading effects. For  $D^{0,\pm}$  production leading effects are weak in SELEX data. E791 and WA92 still show leading behavior for the  $D^-$  but not for  $D^{*-}$ . The SELEX group will continue their pion analysis to try to understand the situation better.

There are many topics in charm hadroproduction left uncovered. In many cases, there are data yet to be analyzed that will address some of the questions. WA92 and WA89 each have published charm total cross sections recently. E791 and SELEX have not yet presented results that will allow us to study the energy and beam particle dependence of charm cross sections. One should expect some results from these groups in

the next year or two.

Having differential distributions for various charm hadrons using different beam particles may allow one to study the effects of the choice of renormalization scale and structure function extrapolation in pQCD calculations. The available data will certainly establish the statistics needed to make such studies profitable.

### 7.1 What do we need to do next?

One of the goals of studying heavy quark (HQ) systems is to test flavor-independence of HQ processes. Are charm cross sections at  $m_T \sim m_b$  the same as b cross sections at the same subenergy? What is the right comparison to make? One now has from E791, for example, good cross section measurements at transverse mass values  $m_T \geq 4$  GeV/ $c^2$ . What b-physics distributions are suitable for comparison? What role does the hadron collider minimum  $p_T$  cut play in complicating the study of flavor independence?

The tests of flavor independence are a specific example of a more general issue in charm hadroproduction - how important is it to have different beam hadrons available for further development of our understanding of hadroproduction? Are collider protons good enough? What are the important physics questions for COMPASS?

We have made great progress in 2 decades of vertex-detector fixed target experiments. Fixed target charm experiments are now largely over, at least for this generation of machines. We now look toward the hadron colliders for charm studies, along with b-quark physics and high- $p_T$  explorations.

## References

- [1] P. Nason, these proceedings
- [2] BEATRICE Collaboration, M. I. Adamovich *et al.*, *Nucl. Phys. B* **495** (1997) 3
- [3] E791 has recent results on  $D^0$  single-particle distributions and D-pairs, accessible from their web page, <http://ppd.fnal.gov/experiments/e791/welcome.html>
- [4] M. I. Adamovich *et al.*, *Eur. Phys. J. C* **8** (1999) 593
- [5] E781 has recent results for  $D^{0,\pm}$ ,  $\Lambda_c^+$  single particle distributions, accessible from their web page, <http://fn781a.fnal.gov/documentation/publication.html>
- [6] E831 has recent results for photoproduction accessible from their web page, <http://www-focus.fnal.gov>
- [7] M. Mangano, P. Nason and G. Ridolfi, *Nucl. Phys. B* **405** (1993) 507
- [8] T. Sjöstrand, *Comput. Phys. Commun.* **82** (1994) 74
- [9] C. Peterson *et al.*, *Phys. Rev. D* **27** (1983) 105
- [10] O.I. Piskounova, [hep-ph/9904208](http://hep-ph/9904208)  
G.H. Arakelyan and Sh.S. Yeremyan, [hep-ph/9808325](http://hep-ph/9808325)
- [11] T. Gutierrez and R. Vogt, *Nucl. Phys. B* **539** (1999) 189  
S.J. Brodsky, P. Hoyer, C. Peterson, and N. Sakai, *Phys. Lett. B* **93** (1980) 451  
S.J. Brodsky, C. Peterson, and N. Sakai, *Phys. Rev. D* **23** (1981) 2745  
S.J. Brodsky, P. Hoyer, A. H. Mueller, and W.-K. Tang, *Nucl. Phys. B* **369** (1992) 519
- [12] M.I. Adamovich *et al.*, *Nucl. Phys. B* **547** (1999) 3
- [13] G.A. Alves *et al.*, *Phys. Rev. D* **49** (1994) 4317